Near-zero dispersion flattened, low-loss porous-core waveguide design for terahertz signal transmission

Jakeya Sultana,[a] Md. Saiful Islam,[b,*] Javid Atai,[c] Muhammad Rakibul Islam,[a] and Derek Abbott[b]
[a]Islamic University of Technology, Department of Electrical and Electronic Engineering, Gazipur, Bangladesh
[b]University of Adelaide, School of Electrical and Electronic Engineering, Adelaide, Australia
[c]University of Sydney, School of Electrical and Information Engineering, Sydney, Australia

Abstract. We demonstrate a photonic crystal fiber with near-zero flattened dispersion, ultralower effective material loss (EML), and negligible confinement loss for a broad spectrum range. The use of cyclic olefin copolymer Topas with improved core confinement significantly reduces the loss characteristics and the use of higher air filling fraction results in flat dispersion characteristics. The properties such as dispersion, EML, confinement loss, modal effective area, and single-mode operation of the fiber have been investigated using the full-vector finite element method with the perfectly matched layer absorbing boundary conditions. The practical implementation of the proposed fiber is achievable with existing fabrication techniques as only circular-shaped air holes have been used to design the waveguide. Thus, it is expected that the proposed terahertz waveguide can potentially be used for flexible and efficient transmission of terahertz waves. [DOI: 10.1117/1.OE.56.7.076114]

Keywords: optics; photonic crystal fiber; effective material loss; terahertz; dispersion.

Paper 170770 received May 21, 2017; accepted for publication Jul. 12, 2017; published online Jul. 31, 2017.

1 Introduction

The terahertz frequency range 0.1 to 10 THz in the electromagnetic frequency spectrum is notable for its growing number of applications including short-range higher data rate wireless communication,[1] medical imaging,[2] pharmaceutical drug testing,[3] security,[4] biotechnology,[5] sensing,[6] etc. It bridges the gap between the microwave and infrared frequency bands and spans the transition between electrical and optical frequencies. But, due to a number of practical difficulties, the commercial deployment of terahertz systems is still challenging. Many current terahertz transmission systems are bulky and depend largely on free-space propagation. But air moisture degrades the signal quality, thus it is a challenge to improve the signal-to-noise ratio. The design of low-loss terahertz waveguides can be a solution to improve the signal quality for a number of key applications. Thus, researchers have proposed several optical waveguides[7–11] for efficient and flexible transmission of terahertz waves. Most of them are disregarded due to higher loss, lower coupling efficiency, higher absorption, and bulky properties. Recently, porous-core photonic crystal fiber (PCF) has gained much attention due to the ability to create desired transmission properties by design. In a PCF, the air hole diameter, pitch size, and the perfectly matched layer (PML) radius are the freely chosen design parameters. In recent years, various studies using porous-core PCF have been proposed. In 2000, in a single-crystal sapphire fiber, the waveguide propagation of sub-ps terahertz pulses was reported by Jaminson et al.[12] In 2008, a cylindrical hollow core-based metallic waveguide consisting of polystyrene deposited on the inner coating was proposed by Bowden et al.[13] They were able to show a loss <1 dB/m for terahertz wave propagation. Later, a hybrid refractometer-based plasmonic terahertz fiber that features two metallic wires inserted into a porous dielectric cladding was proposed by Markov and Skorobogatiy.[14] Kaijage et al.[15] proposed a porous-core octagonal PCF and showed an effective material loss (EML) of 0.07 cm^{-1}, but the dispersion properties of this fiber were not reported. Hasan et al.[16] proposed a circular PCF and showed an EML of 0.056 cm^{-1} with a dispersion flatness of 0.71 ± 0.18 ps/THz/cm within the frequency range of 1 to 1.8 THz. Islam et al.[17] proposed a hexagonal PCF and showed an EML of 0.066 cm^{-1} with a dispersion variation of 1.06 ± 0.12 ps/THz/cm. In 2016, using the EFG/Stepanov technique, the capability for highly efficient terahertz waveguiding in multimode sapphire crystals was reported by Zaytsev et al.[18] Furthermore, Islam et al.[19] proposed a rotated hexagonal PCF and reduced the EML to 0.053 cm^{-1}, but with a large dispersion variation of 1.20 ± 0.25 ps/THz/cm within the frequency range of 1 to 1.55 THz. Later, researchers[20] proposed a modified octagonal PCF and reduced the EML to 0.047 cm^{-1} with a dispersion variation of 1.95 ± 0.15 ps/THz/cm within a short frequency range of 0.95 to 1.25 THz. Recently, a hybrid core PCF has been proposed by Islam et al.[21] which shows an EML of 0.040 cm^{-1} with a dispersion variation of 1.25 ± 0.10 ps/THz/cm within a very short frequency range of 0.95 to 1.15 ps/THz/cm. The above-cited studies indicate that there is a significant possibility for the development of terahertz waveguide designs considering the dispersion and loss.

In this paper, a Topas-based PCF consisting of a hybrid structure in the core and a conventional hexagonal structure in the cladding has been proposed. The resulting proposed PCF shows a near-zero flattened dispersion, ultralow EML, and negligible confinement loss in a broad frequency range. In addition, ease of fabrication is supported via use of

*Address all correspondence to: Md. Saiful Islam, E-mail: mdsaiful.islam@adelaide.edu.au

0091-3286/2017/$25.00 © 2017 SPIE

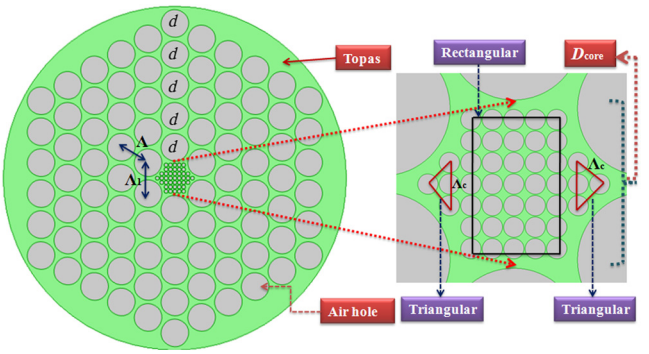

Fig. 1 Schematic diagram of the proposed waveguide.

a typical hexagonal structure with all circular air holes. Modified total internal reflection guides the light throughout the fiber so that perturbations due to external surroundings can be neglected.

2 Design Methodology

Figure 1 shows the schematic cross section of the proposed waveguide. The entire mesh consists of 18,613 boundary elements, 548 vertex elements, and the minimum element quality is 0.04255. In Fig. 1, Λ indicates the spacing between two adjacent air holes in two adjacent rings whereas Λ_1 represents the spacing of two adjacent air holes in the same ring. Note that Λ and Λ_1 are related to one another by $\Lambda_1 = 0.95\,\Lambda$. For the core region, the distances are named as Λ_c. The diameter of air holes in the cladding is denoted by d. Maximum possible air filling fraction d/Λ of 0.95 has been used for a better confinement factor and also to make the dispersion properties flat. Meanwhile, porosity determines the variation of core air holes that can be defined as the ratio of air hole area to the total area of the core. Note that Λ_c is related to Λ by a factor of 7.5. Due to some unique and useful characteristics suitable for terahertz transmission, cyclic olefin copolymer Topas has been chosen as the base material for the proposed PCF. Throughout the simulation, the frequency-dependent character of the absorption coefficient of TOPAS is used. The inherent characteristics include: (i) constant index of refraction ($n_{mat} = 1.525$) over a broad frequency range of 0.1 to 1.5 THz,[22] (ii) suited for biosensing,[23] (iii) lower material absorption loss varies in the range of about 0.1 to 2.0 dB/cm in the frequency range of 0.1 to 1.5 THz, (iv) high glass transition temperature T_g,[24] and (v) negligible hygroscopicity.[25]

3 Results and Discussion

The key propagation properties of the proposed waveguide have been investigated using the full-vector finite element method-based commercially available software package COMSOL version 4.3b. The main concern of the proposed waveguide is to reduce the EML and flatten the dispersion properties. To achieve this goal, it has been possible to use a maximum porosity of 83% because any further increment in porosity may result in overlapping air holes, making fabrication a challenge. After that, the porosity values are changed to a lower level (73% and 63%) to observe the characteristics of the fiber at lower porosities. An antireflective layer that is also known as PML has been used at the outer boundary of the waveguide. The radius of the PML has been set to 9% of the total fiber radius. The values of PML were pretested before starting the final simulation. Actually, we set it to 9% to make the fabrication possibilities easier. If we set it much lower, it could be a problem during fabrication. The electric field distribution of the proposed waveguide is shown in Fig. 2 which confirms the single-mode operation of the proposed PCF.

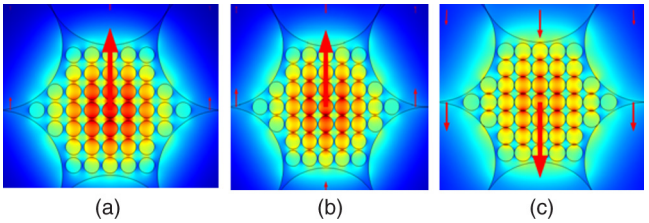

Fig. 2 E-field distribution of the proposed PCF for (a) 63%, (b) 73%, and (c) 83% porosity.

Dispersion is one of the factors that limit the quality of signal transmission over optical links. For a single-mode optical links, dispersion can occur either for the used bulk material (material dispersion) or for the physical structure of the waveguide (waveguide dispersion). But in Topas, the material absorption loss is negligible[22] so only waveguide dispersion has been considered for our proposed fiber. Dispersion mostly depends on the effective refractive index variation of the waveguide with respect to frequency. The dispersion should be as low as possible because if the pulse broadening of optical signals increases the bits of adjacent slots can overlap which may increase the bit error rate. Pulse broadening of a single-mode PCF can be calculated as[26]

$$\beta_2 = \frac{2}{c}\frac{dn_{\text{eff}}}{dw} + \frac{w}{c}\frac{d^2 n_{\text{eff}}}{dw^2}, \text{ps/THz/cm}, \quad (1)$$

where w is the angular frequency, c is the speed of light into free space, and n_{eff} is called the effective refractive index of the material. Figure 3 indicates that a near-zero ultraflattened dispersion is obtained within the frequency range of 0.67 to 1.22 THz. The obtained dispersion variation is 0.6 ± 0.05 ps/THz/cm which is the best (to the best of our knowledge) in the terahertz regime as compared to any previously proposed terahertz waveguide. It is also found that for a broad frequency range 0.6 to 1.6 THz the dispersion

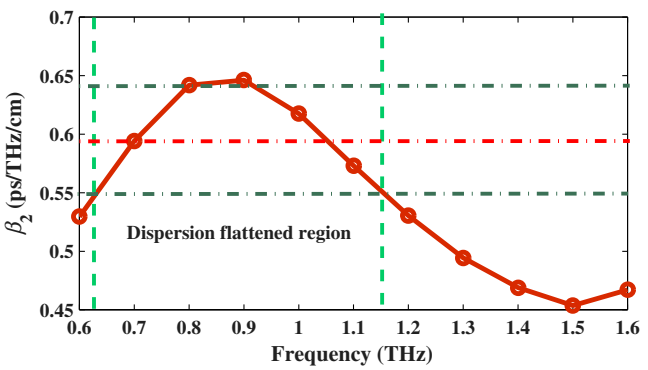

Fig. 3 Characteristics of dispersion variation with frequency at 83% porosity.

variation is 0.52 ± 0.09 ps/THz/cm which is useful for long distance terahertz signal transmission. When a light pulse propagates along the fiber, the guided mode experiences some undesirable losses. This is because a number of polymer materials are lossy. The most important effect to be considered is the material absorption loss or EML. The material absorption loss of a fiber can be quantified as[26]

$$\alpha_{\text{eff}} = \sqrt{\frac{\epsilon_0}{\mu_0}}\left(\frac{\int_{\text{mat}} n_{\text{mat}}|E|^2\alpha_{\text{mat}}\text{d}A}{|\int_{\text{all}} S_z\text{d}A|}\right), \tag{2}$$

where ϵ_0 is the relative permittivity, μ_0 is defined as relative permeability into free space, α_{mat} is the bulk absorption loss, n_{mat} is the refractive index of Topas, and $S_z = \frac{1}{2}(E \times H^*)z$ can be defined as the z component of Poynting vector, where E and H^* are the complex conjugate of the electric field and magnetic field components, respectively. At 1-THz frequency, the characteristics of EML with respect to D_{core} are shown in Fig. 4. It can be observed that EML decreases with the increase of porosity because increased porosity means enlarging the air hole diameter inside the core, thus trimming down the amount of material which in consequence reduces the EML. At optimum design parameters, the obtained EML is 0.03 cm^{-1} which is improved over previously proposed[12–21] waveguides.

Confinement loss of an optical link is also a critical factor that limits the propagation length of the transmitted signal through the terahertz waveguide. Confinement loss has a direct relationship with the number of air holes used, the spacing between adjacent air holes, and the number of rings in the cladding.[27] It approaches zero if the number of air holes in the cladding is infinite. In practice, to make the design simple, the number of air holes in the cladding should be finite. Confinement loss should be as low as possible because if it becomes larger, the propagation length of terahertz PCF will be smaller. It can be calculated as[26]

$$L_c = 8.686\left(\frac{2\pi f}{c}\right)\text{Im}(n_{\text{eff}})\text{dB/cm}, \tag{3}$$

where $\text{Im}(n_{\text{eff}})$ indicates the imaginary part of the complex refractive index, f is the operating frequency, and c is the speed of light into free space. At 1-THz frequency, the amount of confinement loss with respect to D_{core} is shown in Fig. 5. It can be seen that confinement loss is boosted down with the decrease of porosity because such decrements cause an increment of the index difference between the core and cladding that increases the value of the imaginary part of the complex refractive index which in consequence reduces the confinement loss.

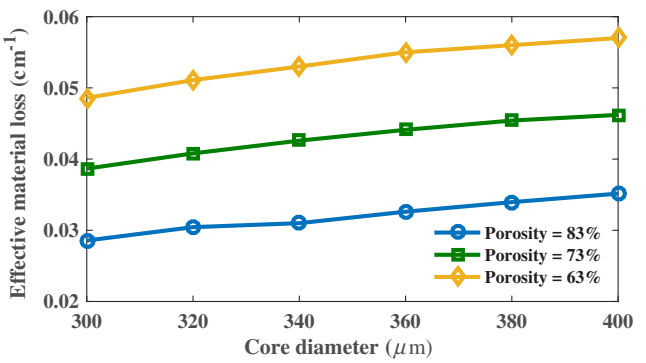

Fig. 4 Characteristics of EML versus D_{core} at different porosities.

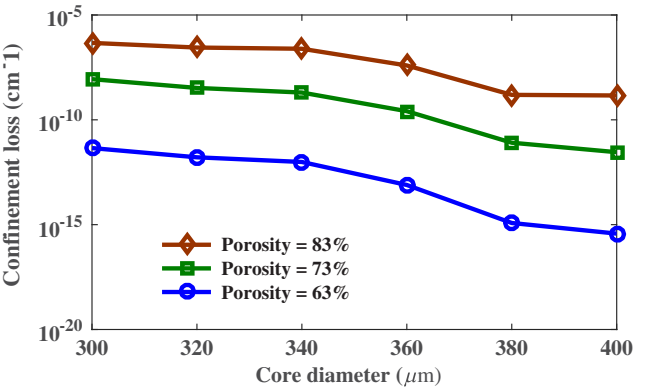

Fig. 5 Characteristics of confinement loss versus D_{core} at different porosities.

We considered 340 μm and 83% porosity as an optimum operating point considering both EML and confinement loss because at this point the obtained EML is 0.03 cm^{-1} which is 85% lower than the bulk absorption loss of Topas and also the obtained confinement loss is negligible which is calculated as $10^{-6.5}$ cm^{-1}.

Now the frequency response of both EML and confinement loss has been investigated in Fig. 6. From Fig. 6, it can be observed that the EML increases linearly with frequency which meets the theoretical consequences of calculating EML using the empirical equation, $\alpha(\nu) = \nu^2 + 0.63\nu - 0.13(\text{dB/cm})$. This is because the electromagnetic wave frequency is proportional to the EML.[21] The EML is lower at a 0.6-THz frequency but we ignore that point because of the higher confinement loss than that of 1 THz. At optimum design parameters and 1-THz frequency, the obtained EML is 0.03 cm^{-1} and obtained confinement loss is $10^{-6.5}$ cm^{-1}. Terahertz PCF with such lower confinement loss characteristics can be suitable for terahertz functional applications, mainly in the terahertz integration systems. Figure 6 shows that as the frequency increases confinement loss reduces because with the increase of frequency the mode powers begins to compress in the core area. So, at optimum design parameters, the obtained EML and confinement loss are clearly improved over earlier proposed[12–21] terahertz optical waveguides.

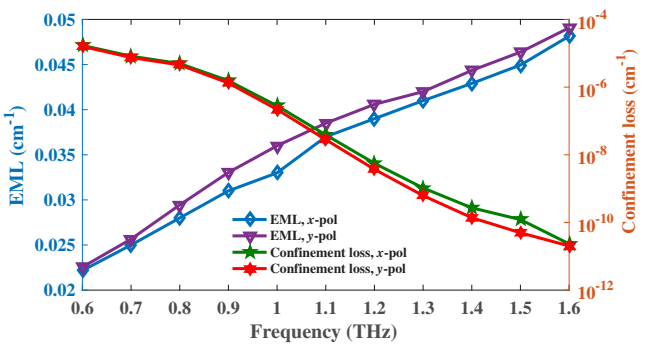

Fig. 6 EML and confinement loss versus frequency at $D_{\text{core}} = 340$ μm and 83% core porosity.

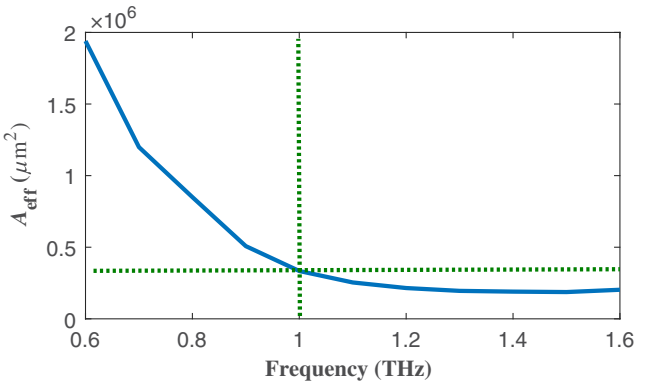

Fig. 7 Characteristics of modal effective area with respect to frequency.

It is also necessary to quantitatively measure the area covered by the proposed waveguide. It can be calculated as[21]

$$A_{\text{eff}} = \frac{[\int I(r) r \mathrm{d}r]^2}{[\int I^2(r) \mathrm{d}r]^2}, \tag{4}$$

where $I(r) = |E_t|^2$ is defined as the electric field intensity and r is the core radius. Figure 7 shows the characteristics of the modal effective area as a function of frequency. It can be observed from the same figure that the modal effective area decreases with the increase of frequency. Because as the frequency increases, less light is being confined in the porous-core area.[21] At the optimal design parameters, a higher effective area of 0.4×10^6 μm^2 is obtained for our proposed fiber.

For the transmission of a signal into longer distances, the light pulses need to be propagated through a single-mode fiber. The single-mode conditions of a fiber can be quantified as[26]

$$V = \frac{2\pi f}{c} \sqrt{n_{\text{co}}^2 - n_{\text{cl}}^2} \leq 2.405, \tag{5}$$

where n_{cl} is the cladding refractive index and n_{co} represents the value of the core refractive index. From Eq. (5), it can be observed that in order to maintain single-mode operations, the value of the V-parameter must be less than or equal to 2.405. Figures 8–10 indicate that the proposed PCF meets the condition of single-mode operation.

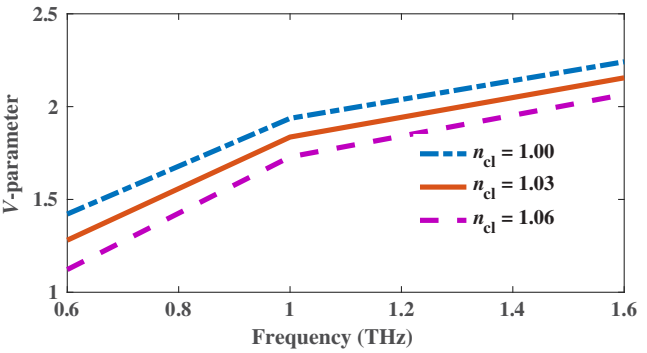

Fig. 8 V-parameter versus frequency at $D_{\text{core}} = 340$ μm and 63% core porosity.

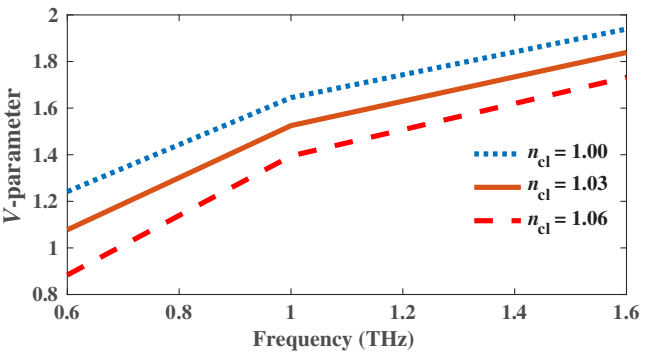

Fig. 9 V-parameter versus frequency at $D_{\text{core}} = 340$ μm and 73% core porosity.

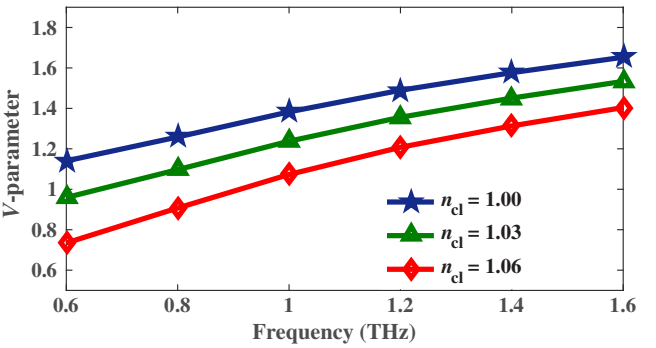

Fig. 10 V-parameter versus frequency at $D_{\text{core}} = 340$ μm and 83% core porosity.

Fabrication must be addressed for practical implementation of this multifunctional proposed waveguide. Considering this fact, we made the design very simple using only circular-shaped air holes. From the technological point of view, the key design parameters are its core porosity, core pitch, core diameter, frequency, etc. These parameters are adjusted in such a way so that the air holes should not overlap with each other because such overlapping may create fabrication difficulties. There are several well-developed ways of fabricating PCFs such as drawing,[22] additive manufacturing (three-dimensional printing),[28,29] capillary stacking,[30] and sol–gel[31] techniques. Microstructured circular-shaped air holes can easily be fabricated using the well-known capillary stacking and sol–gel techniques. Moreover, using capillary stacking and sol–gel techniques, the dimensions of the PCF can be easily adjusted. In addition, a technique designed by Kiang et al.[32] can fabricate almost all types of complex fiber structures.

4 Conclusions

A porous-core PCF has been designed and characterized for efficient terahertz wave transmission. The key findings of the proposed waveguide are its simplicity in design, near-zero flattened dispersion of 0.6 ± 0.05 ps/THz/cm over a broad frequency range of 0.67 to 1.22 THz, ultralower EML of 0.03 cm^{-1}, and negligible confinement loss of the order of $10^{-6.5}$ cm^{-1}. Thus, it is anticipated that if the proposed waveguide can be implemented practically using the state-of-the-art technology, it will play a vital role in those fields that require near-zero flattened dispersion and ultralow-loss

properties and thus play a vital role for practical implementation and commercialization of terahertz waves.

References

1. T. Nagatsuma, G. Ducournau, and C. C. Renaud, "Advances in terahertz communications accelerated by photonics," *Nat. Photonics* **10**(6), 371–379 (2016).
2. C. B. Reid et al., "Accuracy and resolution of THz reflection spectroscopy for medical imaging," *Phys. Med. Biol.* **55**(16), 4825–4838 (2010).
3. K. Kawase et al., "Non-destructive terahertz imaging of illicit drugs using spectral fingerprints," *Opt. Express* **11**(20), 2549–2554 (2003).
4. D. J. Cook, B. K. Decker, and M. G. Allen, "Quantitative THz spectroscopy of explosive materials," in *Proc. of OSA Conf. on Optical Terahertz Science and Technology*, pp. 1–4 (2005).
5. M. Nagel et al., "Integrated THz technology for label-free genetic diagnostics," *Appl. Phys. Lett.* **80**(154), 154–156 (2002).
6. D. Abbott and X. C. Zhang, "Scanning the issue: t-ray imaging, sensing, and retection," *Proc. IEEE* **95**(8), 1509–1513 (2007).
7. D. Qu, D. Grischkowsky, and W. Zhang, "Terahertz transmission properties of thin subwavelength metallic hole arrays," *Opt. Lett.* **29**(8), 896–898 (2004).
8. K. Wang and D. M. Mittleman, "Metal wires for terahertz waveguiding," *Nature* **432**, 376–379 (2004).
9. A. Hassani, A. Dupuis, and M. Skorobogatiy, "Porous polymer fibers for low-loss terahertz guiding," *Opt. Express* **16**(9), 6340–6351 (2008).
10. M. Skorobogatiy and A. Dupuis, "Ferroelectric all-polymer hollow Bragg fibers for terahertz guidance," *Appl. Phys. Lett.* **90**(11), 113514 (2007).
11. S. Atakaramians et al., "Terahertz dielectric waveguides," *Adv. Opt. Photonics* **5**(2), 169–215 (2013).
12. S. P. Jaminson, R. W. McGowan, and D. Grischkowsky "Single-mode waveguide propagation and reshaping of sub-ps terahertz pulses in sapphire fibers," *Appl. Phys. Lett.* **76**(15), 1987–1989 (2000).
13. B. Bowden, J. A. Harrington, and O. Mitrofanov, "Low-loss modes in hollow metallic terahertz waveguides with dielectric coatings," *Appl. Phys. Lett.* **93**(18), 181104 (2008).
14. A. Markov and M. Skorobogatiy, "Hybrid plasmonic terahertz fibers for sensing applications," *Appl. Phys. Lett.* **103**(18), 181118 (2013).
15. S. F. Kaijage, Z. Ouyang, and X. Jim, "Porous-core photonic crystal fiber for low loss terahertz wave guiding," *IEEE Photonics Technol. Lett.* **25**(15), 1454–1457 (2013).
16. M. I. Hasan et al., "Ultra-low material loss and dispersion flattened fiber for THz transmission," *IEEE Photonics Technol. Lett.* **26**(23), 2372–2375 (2014).
17. R. Islam et al., "Low-loss rotated porous core hexagonal single-mode fiber in THz regime," *Opt. Fiber Technol.* **24**, 38–43 (2015).
18. K. I. Zaytsev et al., "Terahertz photonic crystal waveguides based on sapphire shaped crystals," *IEEE Trans. Terahertz Sci. Technol.* **6**(4), 576–582 (2016).
19. M. S. Islam et al., "Porous core photonic crystal fiber for ultra-low material loss in THz regime," *IET Commun.* **10**(16), 2179–2183 (2016).
20. S. Islam et al., "Extremely low-loss, dispersion flattened porous-core photonic crystal fiber for terahertz regime," *Opt. Eng.* **55**(7), 076117 (2016).
21. M. S. Islam et al., "Ultra low loss hybrid core porous fiber for broadband applications," *Appl. Opt.* **56**(9), 1232–1237 (2017).
22. K. Nielsen et al., "Bendable, low-loss TOPAS fibers for the terahertz frequency range," *Opt. Express* **17**(10), 8592–8601 (2009).
23. G. Emiliyanov et al., "Localized bio-sensing with TOPAS microstructured polymer optical fiber," *Opt. Lett.* **32**(5), 460–462 (2007).
24. C. Markos et al., "High-T_g TOPAS microstructured polymer optical fiber for fiber Bragg grating strain sensing at 110 degrees," *Opt. Express* **21**(4), 4758–4785 (2013).
25. J. Balakrishnan, B. M. Fischer, and D. Abbott, "Sensing the hygroscopicity of polymer and copolymer materials using terahertz time-domain spectroscopy," *Appl. Opt.* **48**(12), 2262–2266 (2009).
26. M. S. Islam et al., "Extremely low material loss and dispersion flattened TOPAS based circular porous fiber for long distance terahertz wave transmission," *Opt. Fiber Technol.* **34**, 6–11 (2016).
27. H. Ademgil, "Highly sensitive octagonal photonic crystal fiber based sensor," *Optik* **125**(20), 6274–6278 (2014).
28. R. K. Patel et al., "Spectroscopy: gain spectroscopy of solution-based semiconductor nanocrystals in tunable optical microcavities," *Adv. Opt. Mater.* **4**(2), 187–335 (2016).
29. "e-Manufacturing Solutions additive manufacturing," https://www.eos.info/en (7 July 2017).
30. M. I. Hasan et al., "Design of hybrid photonic crystal fiber: polarization and dispersion properties," *Photonics Nanostruct. Fundam. Appl.* **12**(2), 205–211 (2014).
31. R. T. Bisen and D. J. Trevor, "Sol–gel-derived micro-structured fibers: fabrication and characterization," in *Optical Fiber Communication Conf., Technical Digest (OFC/NFOEC)* (2005).
32. K. M. Kiang et al., "Extruded single mode non-silica glass holey optical fibres," *Electron. Lett.* **38**(12), 546–547 (2002).

Jakeya Sultana received her BSc Engg degree in electronics and telecommunication engineering from Rajshahi University of Engineering and Technology (RUET), Bangladesh, in 2014. She is continuing her MSc Engg degree in electrical and electronic engineering from Islamic University of Technology (IUT). She joined the Department of Electrical and Electronic Engineering, Bangladesh University, in 2016 and is serving as a lecturer there. Her research interests include optical fiber communication, terahertz, optical waveguide design, wireless communication, etc.

Md. Saiful Islam received his BSc Engg degree in electronics and telecommunication engineering from RUET, Bangladesh, in 2012. He received his MSc Engg degree in electrical and electronic engineering from IUT, Bangladesh, in 2016. He is a PhD student in the School of Electrical and Electronic Engineering, University of Adelaide, Australia. His research interests include optical fiber communication, terahertz, optical waveguide design, etc.

Javid Atai obtained his BSc degree in mathematics and physics from the University of Western Australia in 1991 and his PhD in optical physics from Australian National University in 1995. He took up a postdoctoral position with the University of Twente. Currently, he is working as an associate professor in the School of Electrical and Information Engineering, University of Sydney. His research interests include optical devices, optical communications, and nonlinear optical phenomena.

Muhammad Rakibul Islam received his BSc Engg and MSc Engg degrees in electrical and electronic engineering from BUET, Bangladesh, in 1998 and 2004, respectively. He also received his MBA degree in marketing from IBA under the University of Dhaka in 2006. He received his PhD in the Department of Electronics and Radio Engineering, Kyung Hee University, Republic of Korea, in 2010. His research interests include cooperative technique for wireless sensor networks and other wireless applications.

Derek Abbott received his BSc (Hons) degree in physics from Loughborough University in 1982 and a PhD in electrical and electronic engineering from the University of Adelaide in 1995. Since 1987, he has been with the University of Adelaide, where he is currently a full professor in the School of Electrical and Electronic Engineering. He holds over 800 publications/patents. His interests are in the area of multidisciplinary physics and electronic engineering applied to complex systems.